MAX-PLANCK-INSTITUT FÜR PLASMAPHYSIK

GARCHING BEI MÜNCHEN

On the Linear Theory of Drift Tearing

Modes in a Tokamak Plasma

D. Biskamp

IPP 6/163 August 1977

Die nachstehende Arbeit wurde im Rahmen des Vertrages zwischen dem Max-Planck-Institut für Plasmaphysik und der Europäischen Atomgemeinschaft über die Zusammenarbeit auf dem Gebiete der Plasmaphysik durchgeführt.

IPP 6/163

D. Biskamp

On the Linear Theory of Drift Tearing Modes in a Tokamak Plasma

August 1977 (in English)

Abstract

The drift-tearing instability for $m \geq 2$ is reexamined, using two-fluid equations in a cylindrical tokamak plasma. Ion viscosity and a radial plasma flow are included. The method consists of numerically integrating the linearized equations in time. Strong deviations from the analytic dispersion relation are found in the most interesting regime $\omega_e^* > \gamma_T$ for realistic values of η and ω_e^*, the growth rates increasing with ω_e^*. For an inward radial plasma flow stabilization of the tearing mode occurs while an outward drift further increases the growth rate.

I. Introduction

Tearing modes, or resistive kink modes appear to play an important role in tokamak plasmas and have therefore attracted much theoretical interest in recent years. Stability diagrams for the $m \geq 2$ tearing modes in a cylindrical tokamak have been given for typical current distributions [1], and it is shown that for appropriately tailored current profiles tearing instabilities can be completely avoided [2]. Toroidal curvature and compressibility may also have a strong stabilizing effect on resistive modes [3][4].

In a hot, magnetically confined plasma diamagnetic drift-effects have to be taken into account. It has already been shown [5] that in the most important regime of large diamagnetic drift frequency drift-modes couple to tearing modes and growth rates may be substantially reduced. In addition, (ion) viscosity and (electron) thermal conduction are important for tearing modes, as has already been noted by Furth, Killeen, and Rosenbluth [6]. In the present paper we have investigated the properties of drift-tearing modes under the influence of viscosity for small but finite values of η, as has previously been done for the purely resistive tearing instability [7].

In section II an appropriate set of equations is derived. In this model only collisional magnetic viscosity explicitly contributes from the full viscosity tensor, as shown in section III, and we discuss the magnitude of resistivity η, viscosity μ, and drift frequency ω^* for typical tokamak plasmas. In section IV we give numerical results on complex eigenfrequencies and eigenfunctions for different values of ω^*, η, μ. The results differ appreciably from those given in Ref. 5. In section V we consider the effect of an average radial plasma flow.

II. Derivation of model equations

We consider a tokamak plasma in the cylindrical approximation, surrounded by a conducting wall at r = a with an axial periodicity length $2\pi R$. We adopt the so-called tokamak ordering, assuming $\varepsilon = \frac{a}{R} \ll 1$ and safety factor $q(a) \sim 1$, so that $B_\Theta/B_z \sim \varepsilon$, $\delta B_z/\delta B_\Theta \sim \varepsilon$. Taking into account only lowest order terms, we take $B_z = B_o = \text{const.}$ We further assume helical symmetry of the perturbed plasma $f = f(r, m\Theta - kz)$, $k = 1/R$, restricting consideration to toroidal mode number n = 1. From Faraday's law

$$\frac{1}{c}\frac{\partial \underline{B}_\perp}{\partial t} = - \nabla \times \underline{E}$$

one obtains

$$(1) \qquad \frac{1}{c}\frac{\partial \psi}{\partial t} = E_z + \frac{kr}{m} E_\Theta = E_\parallel - \frac{E_\perp \times \nabla z}{B_o} \nabla\psi ,$$

where $\psi(r,\Theta)$ is the helical flux function defined by

$$(2) \qquad \underline{B}_\perp = \nabla z \times \nabla\psi + \frac{kr}{m} B_o \nabla z ,$$

which is conserved for ideal MHD motions.

The parallel field $E_\parallel$ is determined by the parallel component of Ohm's law

$$(3) \qquad \begin{aligned} E_\parallel &= \eta j_\parallel - \frac{1}{n_e} \nabla_\parallel p_e + 0.71 \frac{1}{e} \nabla_\parallel T_e \\ &= \eta j_\parallel - \frac{T_e}{n_e} \nabla_\parallel n , \end{aligned}$$

assuming infinite parallel heat conduction, $\nabla_{\parallel} T_e = 0$, and neglecting electron viscosity. Substitution into eq. (1) yields

$$\frac{\partial\psi}{\partial t} + \underline{v}_E \cdot \nabla\psi = c\eta j_{\parallel} - \frac{cT_e}{ne} \nabla_{\parallel} n$$

(4)

$$\cong c\eta j_z - \frac{cT_e}{eB_o} \frac{1}{n} \nabla z \cdot (\nabla\psi \times \nabla n),$$

with $\underline{v}_E = c\,\underline{E}_{\perp} \times \nabla z/B_o$, $j_z = \nabla^2\psi + 2kB_o/m$.

The parallel plasma velocity will be neglected, $v_{\parallel} \simeq v_z = 0$, because of the large coefficient of parallel viscosity, as will be discussed in the following section. The perpendicular motion is incompressible, because of the slow time scales involved, and also because of viscosity effects. Hence the plasma velocity can be described by a stream function ϕ,

(5) $\underline{v} = \nabla z \times \nabla\phi$.

Taking the curl of the equation of motion,

(6) $\nabla z \cdot \nabla \times (\frac{\partial \rho v}{\partial t} + \nabla \cdot \rho\underline{vv} + \nabla p + \nabla \cdot \underline{\underline{\Pi}} - \frac{1}{c}\,\underline{j} \times \underline{B}) = 0,$

yields an equation for $A = \nabla z \cdot (\nabla \times n\underline{v})$, $n = \rho/m_i$,

(7) $\frac{\partial A}{\partial t} + \underline{v} \cdot \nabla A + \nabla z \cdot (\nabla n \times \nabla\frac{v^2}{2}) = \frac{1}{c} \nabla z \cdot (\nabla\psi \times \nabla j_z) - \frac{1}{m_i} \nabla z \cdot \nabla \times \nabla \cdot \underline{\underline{\Pi}}$

$$\nabla \cdot n\nabla\phi = A.$$

The variation of the density is given by the continuity equation

$$\frac{\partial n}{\partial t} + \nabla \cdot n\underline{v} = 0. \tag{8}$$

We have still to relate the plasma velocity $\underline{v}$ to $\underline{v}_E$ in eq. (4). This is done by using the quasineutrality conditions $\nabla \cdot \underline{j} = 0$,

$$\nabla \cdot \underline{v}_{e\perp} n = \nabla \cdot \underline{v} n + \frac{1}{e} \nabla_{\parallel} j_{\parallel} \tag{9}$$

The perpendicular part of Ohms's law provides a relation between $\underline{v}_E$ and $v_{e\perp}$ (neglecting $\eta j_{\perp}$ since $j_{\perp} << j_z$)

$$\underline{v}_{e\perp} = \underline{v}_E + \underline{v}_e^* ,$$

where

$$\underline{v}_e^* = - \frac{c}{en} \frac{\nabla z \times \nabla p_e}{B_o}$$

are the electron and ion diamagnetic drift velocities. Since $\nabla \cdot n\underline{v}^* = 0$, the diamagnetic drifts do not contribute in eq. (9).

When linearized, eq. (9) can readily be solved for v_E, assuming a cylindrical equilibrium $\psi_o(r)$, $j_o(r)$, $n_o(r)$ and a Fourieransatz $e^{im\Theta}$ in the perturbation. Writing $\underline{v} = \underline{v}_{io}^* + \underline{v}_1$, $\nabla \cdot v_1 = 0$, and leaving off the subscript 1 in the perturbed quantities for simplier notation, we obtain

$$\underline{v_E} = \underline{v} + \frac{1}{e} \nabla_{\parallel} j_{\parallel} \frac{1}{n_o'} \nabla r + h \nabla \Theta \tag{10}$$

$$h = \frac{i}{m} r \frac{\partial}{\partial r} \left(r \frac{\nabla_{\parallel} j_{\parallel}}{e\, n_o'}\right) ,$$

only v_{E_r} being required in the linearized version of eq. (4).

It is convenient to write the equations in dimensionless form by introducing as units the plasma radius a, a typical poloidal Alfvén velocity v_A, poloidal field $B_{\Theta o}$ and density n_o. Temperatures are measured in units of $B^2_{\Theta o}/4\pi n_o$. We have, furthermore,

$$(11) \qquad \eta \rightarrow \frac{\eta c^2}{4\ a v_A} = \frac{\tau_A}{\tau_s}$$

which we continue to call η, and

$$(12) \qquad \frac{1}{e} \rightarrow \frac{c}{\omega_{pi} a} \frac{B_{\Theta o}}{B_o} = \alpha,$$

which is the smallness parameter associated with diamagnetic drifts. Linearization of eqs. (4), (7) and (8) and substitution of v_E using eq.(10) yield the following set of equations

$$(13) \quad \frac{\partial \psi}{\partial t} = \frac{im}{r} \psi_o' \phi + \eta \nabla^2 \psi - \alpha \frac{im}{r} \left[\frac{\psi_o'^2}{n_o'} \nabla^2 \psi - \frac{\psi_o' j_o'}{n_o'} \psi + \frac{T_e \psi_o'}{n_o} n - \frac{T_e n_o'}{n_o} \psi \right],$$

$$(14) \quad \frac{\partial n}{\partial t} = \frac{im}{r} n_o' \phi,$$

$$(15) \quad \frac{\partial A}{\partial t} = - \frac{im}{r} v^{*}_{io} A + \frac{im}{r} (\psi_o' \nabla^2 \psi - j_o' \psi) - \frac{1}{m_i} \nabla z \cdot \nabla \times \nabla \cdot \underline{\underline{\Pi}},$$

$$\text{with } A = \frac{1}{r} \frac{\partial}{\partial r} n_o r \frac{\partial \phi}{\partial r} - \frac{m^2}{r^2} n_o \phi.$$

It is worthwhile to mention that in the general nonlinear case the assumptions of both $\nabla \cdot v_E = 0$ and $\nabla \cdot v = 0$ are not compatible with the quasi-neutrality condition eq.(9). This is, because eq.(9) can be written as

$$(\nabla z \times \nabla n) \cdot \nabla u = -\frac{1}{e} \nabla_{\parallel} j_{\parallel}$$

with $v_E - v = \nabla z \times \nabla u$,

which implies the solvability condition

$$(16) \quad \oint \frac{dl}{|\nabla n|} \nabla_{\parallel} j_{\parallel} = 0 ,$$

where the integral is taken along density contours. In general eq.(16) is not satisfied. Consequently one has to relax the incompressibility condition imposed on either v or v_E. Let us consider a somewhat different approach of deriving equations for drift-tearing modes. Instead of using the ion continuity equation (8) we choose the electron continuity equation

$$(17) \quad \frac{\partial n}{\partial t} + v_E \cdot \nabla n = \frac{1}{e} \nabla_{\parallel} j_{\parallel} \qquad \text{(again for } v_{i_{\parallel}} = 0\text{)},$$

which is completely equivalent to (8) for $\nabla \cdot j = 0$. All we need is an equation for v_E. The ion equation of motion yields $v_E = v_i - v_i^* + O(\omega/\Omega_i)$. Since the inertia term in eq.(6) is small we substitute $v_E + v_i^*$ for v which is a good approximation as long as the corresponding frequency $\omega \simeq \omega^*$ is not too large. Instead of the equations (13) - (15) one obtains the following set

$$(13a) \quad \frac{\partial \psi}{\partial t} = \frac{im}{r} \psi_o' + \eta \nabla^2 \psi - \alpha \frac{imT_e}{r\, n_o} \left[\psi_o' n - n_o' \psi \right]$$

$$(14a) \quad \frac{\partial n}{\partial t} = \frac{im}{r} n_o' \phi_E + \alpha \frac{im}{r} \left[\psi_o' \nabla^2 \psi - j_o' \psi \right]$$

$$(15a) \quad \frac{\partial A_\varepsilon}{\partial t} = -\frac{im}{r} v_{io}^* A_E + \frac{im}{r} (\psi_o' \nabla^2 \psi - j_o' \psi) - \frac{1}{m_i} \nabla z \cdot \nabla \times \nabla \cdot \underline{\underline{\Pi}},$$

$$A_E = \left(\frac{1}{r} \frac{\partial}{\partial r} n_o \frac{\partial}{\partial r} - \frac{m^2}{r^2} n_o\right) \phi_E .$$

The difference between (13), (14) and (13a), (14a) is effectively due to a small difference in the definition of v_E. In the standard derivation of the dispersion relation, dicussed in section IV, replacing the set (13) - (15) by (13a) - (15a) amounts to replacing ω_e^* in the second term on the r.h.s. in eq.(24) by ω. Since this term is important only in the regime $\omega \simeq \omega_e^*$ the difference is negligible. Also when using the more accurate procedure of obtaining eigenfunctions and eigenvalues as described in detail in section IV, the difference between both models is small. For numerical convenience we restrict the detailed evaluations to the model (13) - (15).

The properties of the nonlinear equations will be investigated in a forthcoming paper.

III Ion viscosity and diamagnetic drifts

We assume that the ion stress tensor $\underline{\underline{\Pi}}$ in eq. (7) is determined by the ion-ion collision time τ_i and has the form as given by Braginskii[8]. This is valid for mean free path smaller than parallel wavelength, $v_i \tau_i / Rq < 1$, which is usually satisfied for present day tokamaks. For longer mean free path ion Landau damping would replace ion viscosity, which will not be considered in this paper.

The stress tensor contains three viscosity coefficients differing by many orders of magnitude, 1. the nonmagnetic viscosity μ_o proportional to the ion collision time τ_i; 2. the nondissipative magnetic viscosity or gyroviscosity μ_g, which is independent of τ_i; 3. the collisional magnetic viscosity μ_c proportional to τ_i^{-1}. The parallel component of the equation of motion is, assuming $\nabla \cdot v = 0$,

$$(18) \qquad \frac{\partial v_{\parallel}}{\partial t} = \frac{e}{m_i} E_{\parallel} - \frac{1}{n_o} \nabla_{\parallel} p_i - \frac{\mu_o}{R^2} v_{\parallel}$$

The magnitude of the viscosity is, using our normalization,

$$\frac{\mu_o a}{R^2 v_A} \sim \frac{a^2}{R^2} \frac{v_A \tau_i}{a} \sim 10^2$$

for typical tokamak plasma ($T_i \simeq 400\text{eV}$, $n = 10^{13}$). Thus the l.h.s. of (18) can be neglected, since $\omega \ll 1$. Outside the resistive layer eq. (3) yields $e n_o E_{\parallel} = T_e \nabla_{\parallel} n$, and using eq. (14), $\omega n \sim n_o' v_r$, we obtain the following estimate of $v_{\parallel}$

$$\frac{\omega^*}{\omega} \frac{a \omega_{pi}}{c} v_r \sim 10^2 \quad v_{\parallel},$$

implying

$$v_{\parallel} << v_{\perp}$$

for realistic values of $\frac{a\omega_{pi}}{c}$ discussed below. The μ_o-terms in the perpendicular components of $\underline{\underline{\Pi}}$ vanish because of $\nabla \cdot v_{\perp} = 0$. If, however, toroidal corrections are included, $v_{\perp}$ would no longer be incompressible and instead one would have $\nabla \cdot v_{\perp}/R^2 = 0$ because of the R^{-1} dependence of the toroidal field. In this case μ_o-terms do not cancel and should have a strong influence on the plasma motion [9), 10)]. In the expression $\nabla z \cdot \nabla \times \nabla \underline{\underline{\Pi}}$ the μ_g terms cancel, too, as can easily be shown by direct calculation, and we are thus left with collisional magnetic viscosity only:

$$- \nabla z \cdot \nabla \times \nabla \cdot \underline{\underline{\Pi}} = \mu_c m_i n \left(\nabla^2 + 4 \frac{\partial^2}{\partial z^2}\right) \nabla z \cdot \nabla \times \underline{v}$$

$$\simeq m_i \mu_c \nabla^2 A,$$

where ∇^2 is the two-dimensional Laplacian as before and

$$(19) \quad \mu_c = \frac{3}{10} \frac{T_i}{\Omega_i^2 \tau_i m_i}$$

The coefficient $\underline{\mu_c}$ normalized to $v_A a$ can be expressed in terms of the (dimensionless) resistivity (13):

$$(20) \quad \mu_c = \frac{3 \cdot \sqrt{2}}{10} \beta_e \left(\frac{T_e}{T_i}\right)^{1/2} \left(\frac{m_i}{m_e}\right)^{1/2} \eta$$

$$\simeq \frac{1}{2} \beta \sqrt{\frac{m_i}{m_e}} \eta .$$

For present-day tokamaks with β slightly above 0.1%, $\frac{1}{2} \beta \sqrt{\frac{m_i}{m_e}}$ is somewhat smaller than 0.1, increasing above 0.1 for the next generation of tokamaks with $\beta \gtrsim 0.5$ %. Using these values, collisional magnetic viscosity, though the weakest of the viscosity processes, nevertheless has an appreciable effect on the structure of the drift-tearing modes, as will be seen in section IV.

The coefficient α in eq. (13) characterizes the magnitude of the diamagnetic drifts. The (normalized) drift frequency is given by

$$\omega_e^* = -\alpha \frac{m}{r} \frac{T_e n_o'(r)}{n_o(r)} \quad . \tag{21}$$

Note that in eqs. (13) - (15) only the density gradient appears, but not the temperature gradient, which is eliminated by the assumption of infinite parallel electron heat conduction in eq. (3). Numerical values are $c/\omega_{pi} \simeq 10/\sqrt{n_e}$, where n_e is in $10^{13}cm^{-3}$, and $\frac{B_{\Theta o}}{B_o} = \frac{1}{q}\frac{r}{R} \simeq \frac{1}{15}$, hence

$$\begin{aligned} \alpha &\simeq \frac{2}{3\cdot\sqrt{n}\;\, a} \simeq \frac{1}{30} \text{ for present-day tokamaks,} \\ &\lesssim 10^{-2} \text{ for the next generation of tokamaks.} \end{aligned} \tag{22}$$

Numerical values of the (normalized) resistivity are

$$\begin{aligned} \eta &= 1.3 \times 10^{-5} \frac{R}{a} \frac{q(s)}{s} \frac{n Z_{eff}}{B_o T_e^{3/2}} \quad (B_o \text{ in T, } T_e \text{ in } 10^2 eV) \\ &\simeq 10^{-5} - 10^{-6} \text{ for present-day tokamaks,} \\ &\simeq 10^{-6} - 10^{-7} \text{ for next generation tokamaks.} \end{aligned} \tag{23}$$

The value of η strongly depends on the radial position of the singular surface (T_e effect) and the Z_{eff}. Typical (normalized) tearing-mode growth rates are $\gamma \sim 10^{-3} < \omega^*$, so that strong modifications of the instability by drift effects are to be expected[5) for plasmas of most interest.

IV Dispersion relation of drift-tearing modes

In the conventional theory of the tearing instability the plasma is split into a thin layer around the resonant surface, where nonideal effects are considered in a simple geometry, and an ideal MHD outside region. Matching of the two solutions yields the eigenfrequencies. Within the resistive layer eqs. (13) - (15) are approximated by (neglecting viscosity for simplicity)

$$(\omega - \omega_e^*)\ (\psi + \frac{m}{r}\psi_o' \frac{\phi}{\omega}) = i(\eta + i\frac{\alpha^2(\frac{m}{r})^2\psi_o'^2 T_e}{n_o\omega_e^*})\ \psi'' ,$$

(24)

$$\omega A = \omega_i^* A - \frac{m}{r}\psi_o' \psi'' .$$

These equations agree in essence with those given in Ref. 11. In Ref. 5 the ω_e^* in the damping term adding to η is replaced by ω, which corresponds to model (13a) - (15a), as mentioned in section III.

(25) $$\omega(\omega - \omega_i^*)(\omega - \omega_e^*)^3 = i\gamma_T^5 ,$$

γ_T being the tearing-mode growth rate for $\omega^* \to 0$. Limiting values of ω are (for $\omega_i^* = 0$)

$$\omega = 0.6\ \omega_e^* + i\gamma_T , \quad \omega_e^* << \gamma_T,$$

(26)

$$= \omega_e^* + \frac{1}{2} i\gamma_T (\frac{\gamma_T}{\omega_e^*})^{2/3} , \quad \omega_e^* >> \gamma_T .$$

The solution of (25) is plotted in Fig. 1 for a typical value of γ_T. In a previous paper[7)] we demonstrated that, because of the small fractional powers of η that determine the resistive layer thickness for $m \gtrsim 2$, very small values of η ($\lesssim 10^{-7}$) are required to recover the results of the conventional theory. In the case of drift-tearing modes, where drift waves may propagate outside the resistive layer, a rather "nonlocal" mode structure is to be expected which may further restrict the validity of the splitting technique mentioned above.
To determine the dispersion relation and eigenfunctions, we have therefore used a more general numerical method similar to that used in Ref. 7, which consists of integrating eqs. (13) - (15) in time. After a transient period - several exponentiation times - the most unstable mode is filtered out and its (complex) frequency can be read off. More specifically, the differential equations are transformed to finite difference form using a leap-frog scheme for advancing quantities in time, ψ at n Δt; n, ϕ at $(n + \frac{1}{2})\,\Delta t$. Equation (13) is written in implicit form for ψ to avoid severe restrictions on the time step arising from the $\nabla^2\psi$ terms. Because of the large numerical values the factor $\alpha\psi'^2/n_o'$ may assume, a careful time centering of this term is required. Though the overall difference scheme is not unconditionally stable, the stability condition arising from finite poloidal Alfvén speed $\Delta t < r\sqrt{n_o(r)/m\psi_o'}$ is not restrictive for small poloidal mode number m and finite density $n_o(r)$. As a typical current profile we choose the "rounded model" of Ref. 1,

$$(27) \qquad j_o(r) = \frac{2\sqrt{2}s^5}{(r^4 + s^4)^{3/2}} \quad , \; s = 0.66 \quad .$$

The density profile is $n_o(r) = 0.8\ (1 - r^2)^2 + 0.2$, and the resistivity is $\eta_o(r) = \eta_o j_o(r_s)/j_o(r)$, where r_s is the singular radius. The viscosity is assumed constant across the plasma, $\mu_c = 0.1\ \eta_o$ for most cases, a realistic number as discussed in the previous section. T_e is chosen $T_e(r) = T_e(r_s)(j_o(r)/j_o(r_s))^{2/3}$. Varying T_e corresponds essentially to shifting the ω_e^* scale, which implies that the dispersion relation is determined by αT_e (i.e. ω_e^*) and not by α.

In Fig. 2 we have plotted the growth rate γ as a function of ω_e^* for three values of η_o. Evidently a strong deviation from the analytical result Fig. 1, which corresponds to $\eta_o = 10^{-6}$, occurs for $\omega_e^* > \gamma_T$. This is due to the finite size of the singular radius. For $\omega^* \simeq \gamma_T$ drift waves are localized close to r_s, Fig. 3, propagating away from the resistive layer, where they are damped because of shear. This corresponds to an energy flow out of the "unstable" region leading to a reduction of the growth rate, which is qualitatively the same effect as the shear stabilization of drift-instabilities [12].

For larger ω^* drift waves propagate across the whole plasma, Fig. 4, and boundary effects become important. In the usual case where $\omega^*(r)$ decreases for increasing radius, drift-modes are confined to the interior of the singular surface $0 < r \simeq r_s$. At $r = 0$ boundary conditions are given by the requirement of regularity,

$\phi = n = \psi = 0$. This implies reflection of the drift-wave leading to a standing wave. Energy is thus transported back into the resistive layer reinforcing the tearing instability, which explains the increase of γ. The modulation of the γ curve in this regime, as seen in Fig. 2, is due to the discrete radial wave number effects (small number of nodes).

In the opposite case of radially increasing ω^* the drift-modes would be confined to the exterior region $r_s \lesssim r < 1$. In this case boundary conditions at the wall would play a crucial role. These are strongly depending on the properties of the plasma close to the wall which is probably at least partly absorbing. Since, however, the case $d\omega^*/dr > 0$ is of less practical interest, we have not considered it in detail.

The dependence on the sign of $d\omega^*/dr$ can easily be recovered analytically. Since this is a property of drift-wave propagation, we neglect the η term in eq. (13). Inserting j from eq. (13) into (15) and using $\nabla \cdot (n_o \nabla\phi) \cong n_o \phi''$, we obtain

(28) $$\phi'' - a^2 \Omega \phi = b \frac{\psi}{\omega} ,$$

with
$$a^2 = \frac{1}{\alpha} \frac{m}{r} \left| \frac{n_o'}{n_o} \right| \frac{1}{\omega^2}$$

$$b = \left| \frac{n_o'}{\alpha n_o} \right| \frac{\Omega}{\psi_o'} + \frac{m}{r} \left| \frac{j_o'}{n_o} \right|$$

$$\Omega = \omega - \omega_e^*(r)$$

Neglecting ψ, we find that for $\Omega < 0, \phi$ is oscillatory, while for $\Omega > 0$ it is exponentially decaying. Since $\omega \simeq \omega_e^*(r_s)$, $d\omega^*/dr < 0$ corresponds to $\Omega < 0$ in $0 < r < r_s$ while $d\omega^*/dr > 0$ corresponds to $\Omega < 0$ in $r_s \lesssim r < 1$.

As ω_e^* is increased further, the radial wave number (number of nodes in the eigenfunction) becomes smaller, which increase the radial propagation velocity thus increasing the growth rate. For $\omega \simeq 0.2$ the ϕ and n eigenfunction assume the longest possible wavelength (no nodes in $0 < r < 1$), so that by further increasing ω_e^* the growth rate does not increase, in fact there is a strong reduction.

Figure 2 clearly shows that for $\omega^* > \gamma_T$ the growth rate does not scale as $\gamma \propto \eta$ for fixed ω^* as predicted by eq. (26), but with a much smaller power of η. As mentioned above the reason is the propagation of the drift-modes across the entire plasma $r \lesssim r_s$. This effect is partly due to the large parallel ion viscosity μ_o strongly suppressing parallel ion motion (in our model we assume $v_\parallel = 0$) which can be seen when instead we solve eq. (18) for $\mu_o = 0$, inserting $v_\parallel$ into the continuity equation (14). Figure 5 gives the eigenfunctions for this case for parameters corresponding to those of Fig. 4. For $\omega^* \gtrsim \gamma_T$ drift-modes are more localized to $r \simeq r_s$ region, growth rates remaining smaller than for $v_\parallel = 0$, see the dispersion relation for $\mu_o = 0$, Fig. 6. For larger ω_e^*, eventually the drift-mode again fills the entire region $0 < r \lesssim r_s$ leading to γ

increasing with ω_e^* . Thus parallel ion viscosity in the region outside the resistive layer strongly changes eigenfunctions and growth rates

The effect of the collisional magnetic viscosity μ_c is somewhat weaker, though it has an appreciable influence on the fine structure of the eigenfunctions for $\omega^* \sim \gamma_T$, as shown in Figs. 7 and 8. For higher values of ω^* the effect becomes small.

It is interesting to note the role played by the term proportional to $\nabla_{\parallel} j_{\parallel}$ in v_{Er} , eq. (12), which in the analytic treatment Ref. 10, is taken into account to provide spatial damping of the drift-waves, but does not enter the dispersion relation (25). Leaving out this term would give rise to a completely different "eigenfunction", Fig. 9, with a much larger"growth rate".

V Influence of radial plasma flow

Finite resistivity gives rise to an average radial plasma flow, the magnitude and direction depending on the distribution of particle sources. Usually one has $v_o \gtrsim O(\eta)$. Although this is generally a small velocity comparing v_o/a with the tearing mode growth rate $\gamma \sim \eta^{3/5}$, it may produce a strong effect in the resistive layer, $v_o/\delta \sim \eta^{3/5} \sim \gamma$, δ being the resistive layer width $\delta \sim \eta^{2/5}$. To include this effect, a convective term has to be added on the left hand sides of eqs. (15) to (17). Closer inspection, however, reveals a smaller influence of v_o on the tearing instability than expected from the argument just given. ψ has a finite value at r_s but its derivative is quasi-regular and hence $\partial\psi/\partial r < \psi / \delta$, while n and ϕ, which have singular derivatives, both vanish at r_s and hence the major contribution of the convective terms $v_o \partial\phi/\partial r$, $v_o \partial n/\partial r$ arise in a region of little influence on the instability.

A qualitative estimate of the growth rate can be given, considering th v_o - term only in the ψ - equation:

(29) $$\gamma \simeq \gamma_T + \frac{v_o}{H} , \qquad H^{-1} = - \frac{1}{\psi} \frac{\partial\psi}{\partial r} \Big/_{r_s} ,$$

where H is some positive number which only weakly (logarithmically) depends on η. Since $\gamma_T \simeq \frac{\eta\Delta'}{\delta}$, the velocity necessary to make the system marginaly stable is

(30) $$v_{om} \simeq - \eta \, \Delta' \, \frac{H}{\delta}$$

Hence we expect that an inward flow $v_o \propto \eta^{3/5}$ may stabilize the tearing mode while an outward flow further increases the growth rate (In the case of a symmetric plane current sheath, $\partial\psi/\partial r = 0$, and a plasma flow has no influence on the tearing instability). Numerical calculation of $\gamma(v_o)$ confirms this picture, Fig. 10. Here we have normalized v_o to $\eta\Delta'$. We find that the value of $v_{om}/\eta\Delta'$ increases by a factor of 2.2 when decreasing η from 10^{-6} to 10^{-7} which is consistent with $(10)^{2/5} \simeq 2.5$ predicted by eq.(30). We also confirm that the convective terms $v_o\partial/\partial r$ inserted into eqs. (14), (15) have negligible effect.

It has been observed in tokamaks [13)] that magnetic mode activity is considerably reduced during the phase of central density increase due to gas inflow. This could be related to the stabilizing effect of an inward plasma flow, though a quantitative comparison is difficult.

VI Conclusions

We have derived and solved a set of equations for the tearing instability in a cylindrical tokamak-like plasma within the framework of the two-fluid theory, including the effect of diamagnetic drifts, ion viscosity and radial plasma flow. The method consists in numerically integrating the equations in time to obtain the complex frequency and eigenfunctions of the strongest growing mode, using values of η, ω^* , μ corresponding to present day and next generation tokamaks. The main results are:

a) In the regime $\omega_e^* > \gamma_T$ growth rates differ appreciably from those predicted analytically, being much larger. This is due to drift-waves propagating over the entire plasma interior $r \leq r_s$ and feeding energy back into the resistive layer.

b) If parallel ion viscosity is neglected, parallel ion motion leads to stronger spatial damping of the drift-waves outside the resistive layer and hence smaller growth rates.

c) Collisional magnetic viscosity appreciably affects the mode structure for $\omega^* \sim \gamma_T$, but has little effect for larger drift frequencies.

d) An average radial plasma flow v_o may stabilize or further destabilize the tearing instability if the flow is inward or outward, respectively. The marginal drift velocity scales $v_o = O(\eta^{3/5})$.

The nonlinear development of drift-tearing modes will be investigated in a forthcoming paper.

Acknowledgements

The author would like to thank Mrs. M. Walter for carrying through the numerical computations and Dr. W. Horton for some discussions on drift-wave theory.

References

1) H.P. Furth, P.H. Rutherford, H. Selberg, Phys. Fluids 16, 1054 (1973)

2) A.H. Glasser, H.P. Furth, P.H. Rutherford, Phys. Rev. Letters 38, 234 (1977)

3) A.H. Glasser, J.M. Greene, J.L.Johnson, Phys. Fluids 18, 875 (1975)

4) A.H. Glasser, J.M. Greene, J.L. Johnson Phys. Fluids 19, 567 (1976)

5) P.H. Rutherford, H.P. Furth, MATT-872, Princeton University 1971

6) H.P. Furth, J. Killeen, M.N. Rosenbluth, Phys. Fluids 6, 459 (1963)

7) D. Biskamp, H. Welter, Plasma Physics and Controlled Nuclear Fusion Research 1976, Vol I, 579

8) S.I. Braginskii, Reviews of Plasma Physics, Vol I, 1965, p. 205

9) M.A. Hellberg, N.K. Winsor, J.L. Johnson Phys. Fluids 17, 1258 (1974)

10) H. Tasso, Plasma Physics and Controlled Nuclear Fusion Fusion Research 1976, Vol III, p. 371,

11) B. Basu, B. Coppi, MIT-report, PRR-76/39

12) L.D. Pearlstein, H.L. Berk, Phys. Rev. Letters 23, 220(1969)

13) S. Sesnic, private communication

Figure captions

Fig. 1. Theoretical dispersion relation, eq. 25, for $\omega_i^* = 0$ and $\gamma_T = 4 \times 10^{-3}$, corresponding to $\eta_o \simeq 10^{-6}$.

Fig. 2. Numerical function $\gamma(\omega_e^*)$ for three different values of η_o. Here realistic values $\omega_i^* = \frac{1}{2}\omega_e^*$, $\mu_c = 0.1\ \eta_o$ are chosen.

Fig. 3. Eigenfunctions ψ, Φ, n for $\eta_o = 10^{-7}$, $\omega_e^* = 6 \times 10^{-3}$ $r_s = 0.5$.

Fig. 4. Eigenfunctions ψ, Φ, n for $\eta_o = 10^{-7}$, $\omega_e^* = 1.5 \times 10^{-2}$ $r_s = 0.5$.

Fig. 5. Eigenfunctions for $\mu_o = 0$. $\eta_o = 10^{-6}$, $\omega_e^* = 7 \times 10^{-3}$. For $v_\parallel = 0$ ($\mu_o \to \infty$), the usual case considered, Φ, n would be similar to those of Fig. 4.

Fig. 6. $\gamma(\omega_e^*)$ for $\mu_o = 0$, the remaining parameters corresponding to those of the $\eta_o = 10^{-6}$ case of Fig. 2.

Fig. 7. Eigenfunctions for $\mu_c = 0.03\ \eta_o$, $\eta_o = 10^{-6}$, $\omega_e^* = 1.5 \times 10^{-2}$.

Fig. 8. Eigenfunctions for $\mu_c = 0.3\ \eta_o$, the remaining parameters as in Fig. 7.

Fig. 9. "Eigenfunctions" obtained when neglecting $\nabla_\parallel j_\parallel$ in the quasineutrality condition eq. (9). This term gives rise to the spatial damping of the drift-waves.

Fig. 10. $\gamma(v_o)$ for $\eta_o = 10^{-6}$, 10^{-7} and $\omega_e^* = 0$.

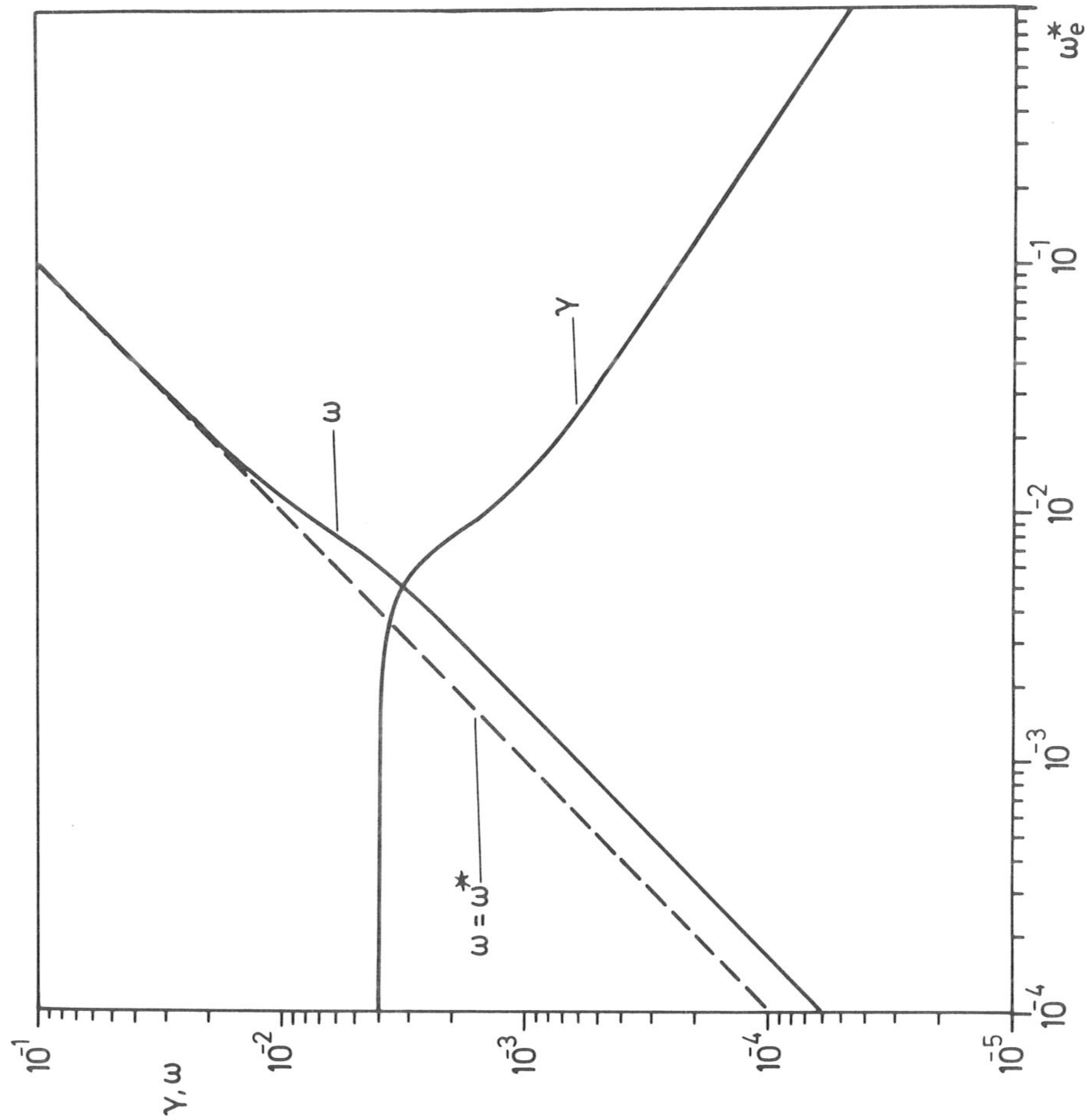

Fig. 1.

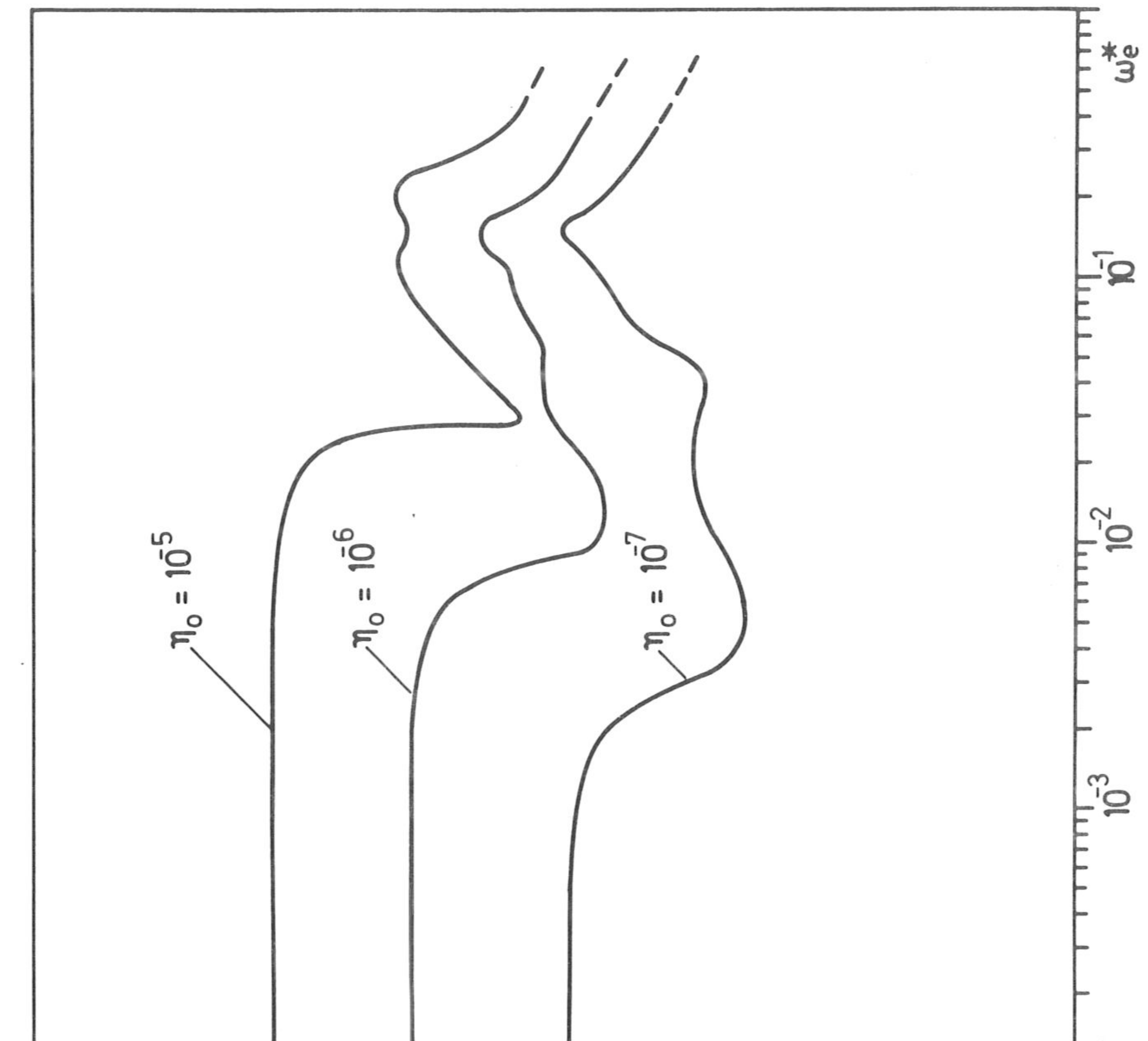

Fig. 2.

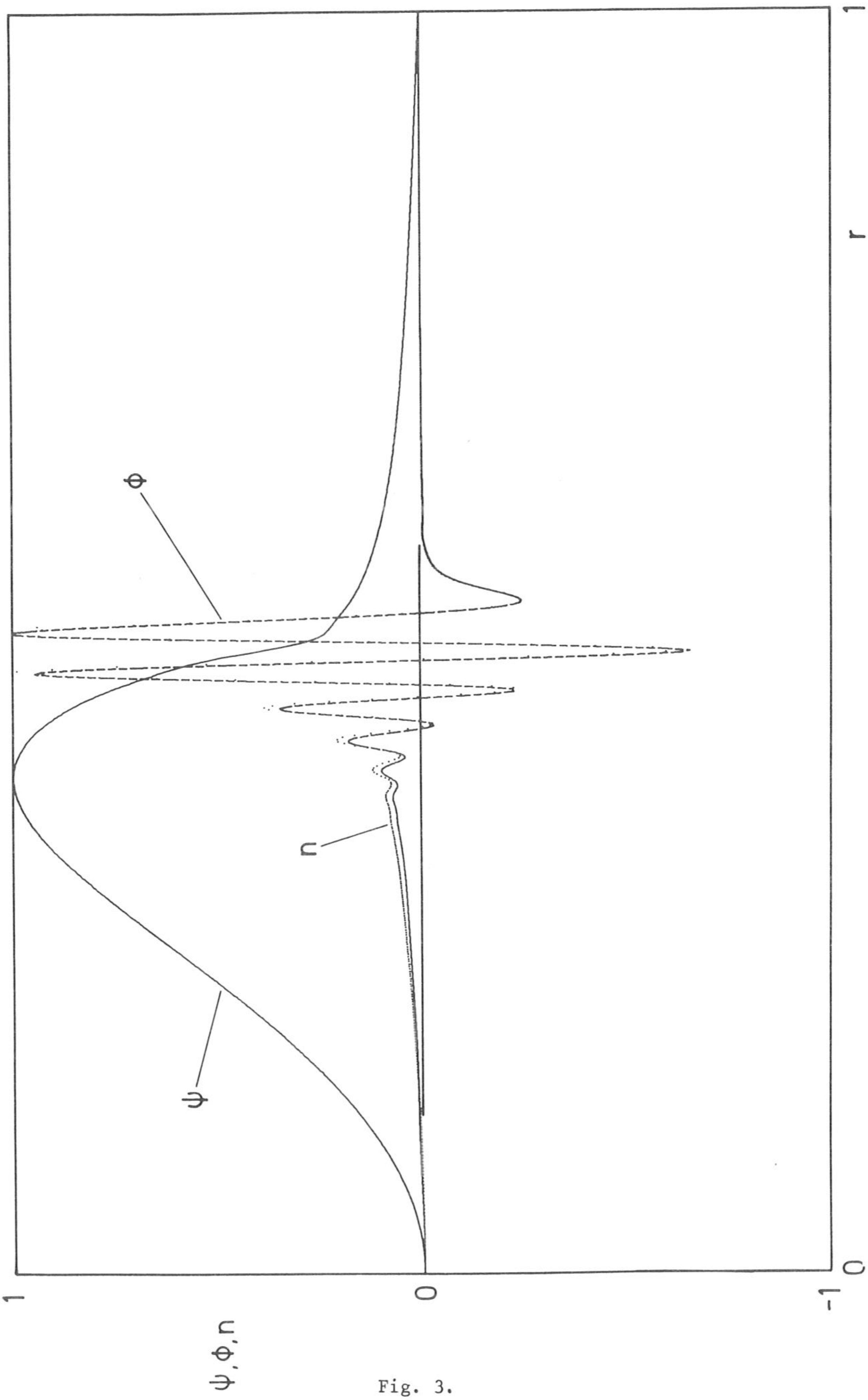

Fig. 3.

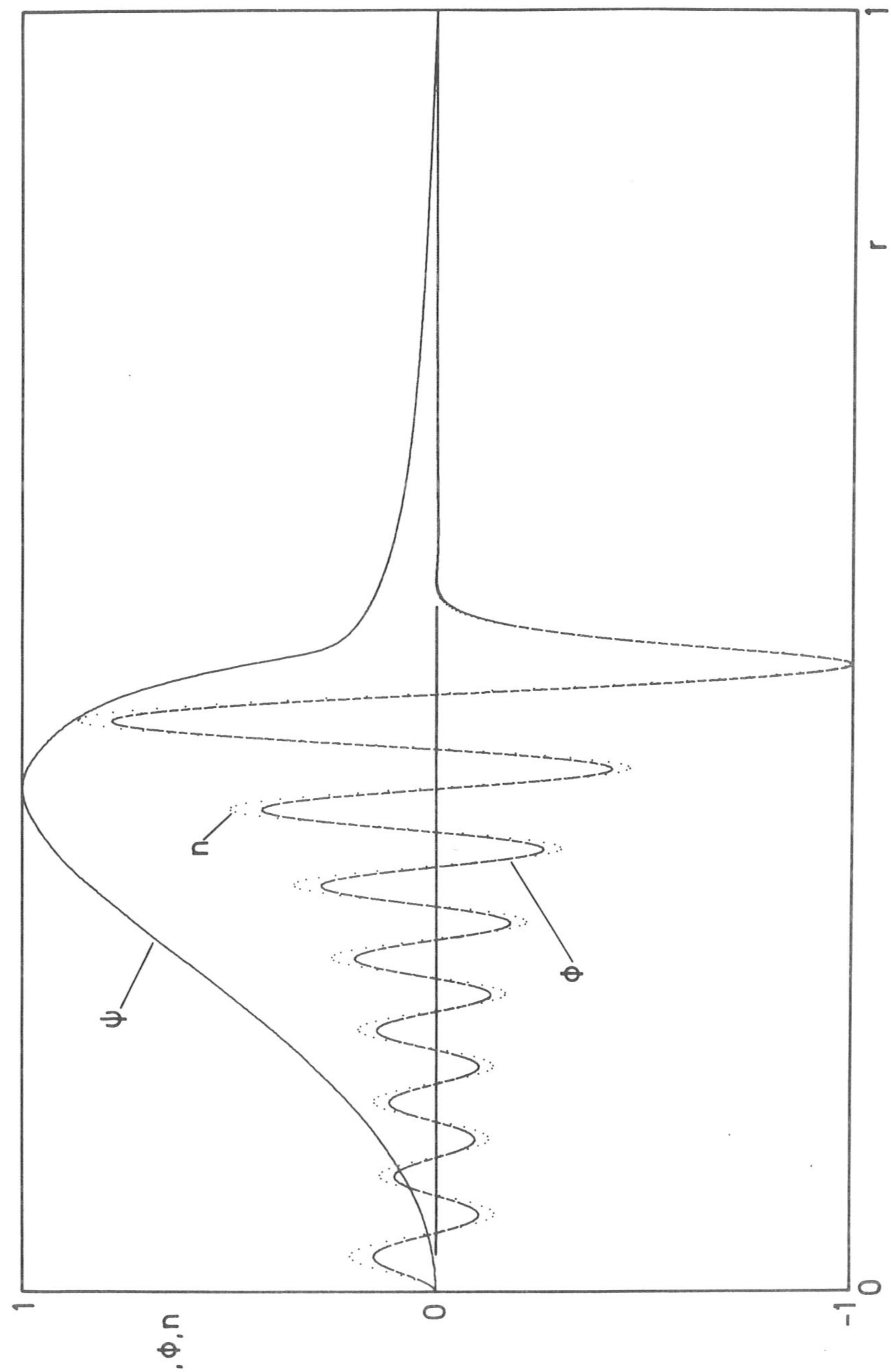

Fig. 4.

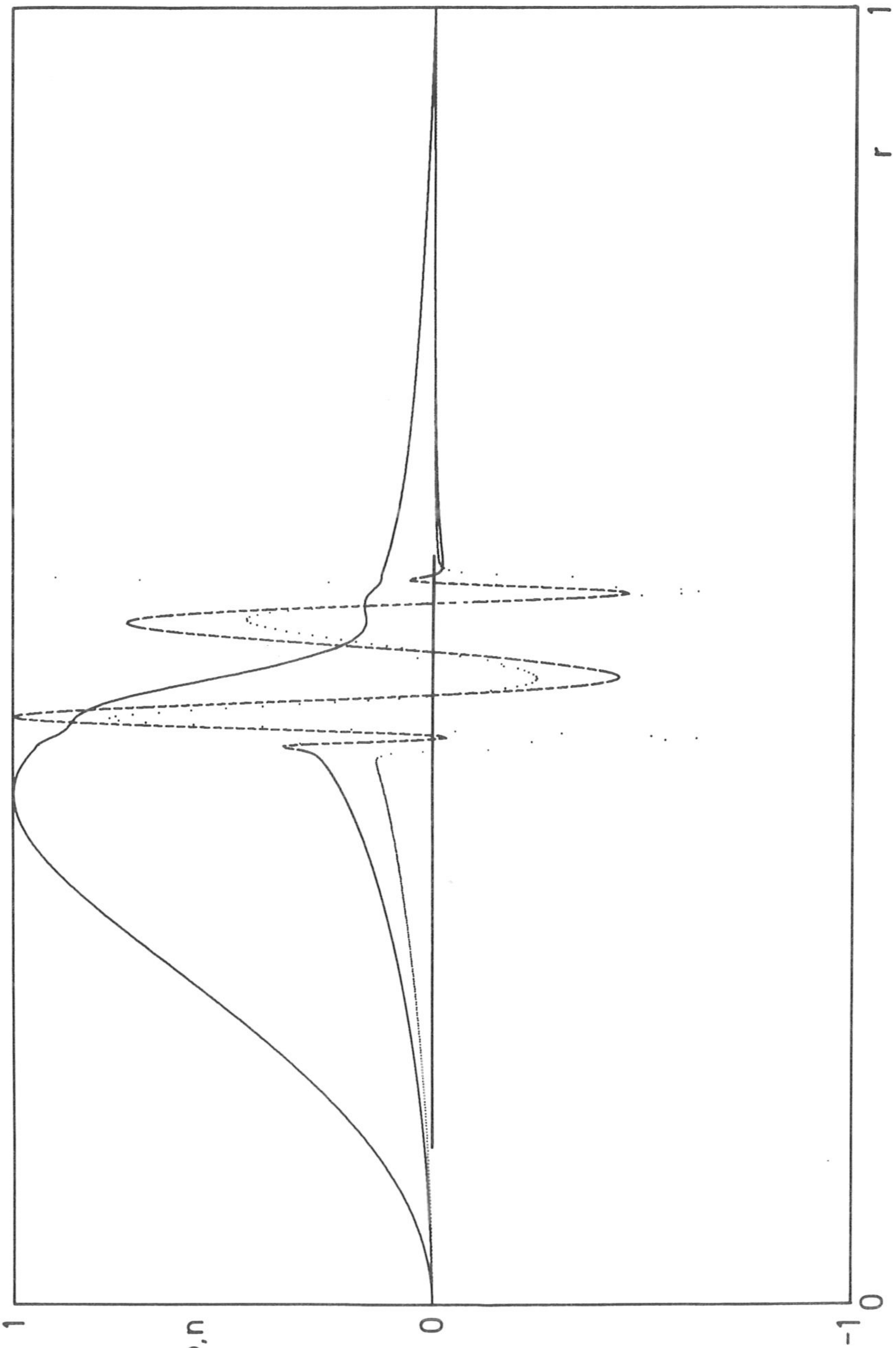

Fig. 5.

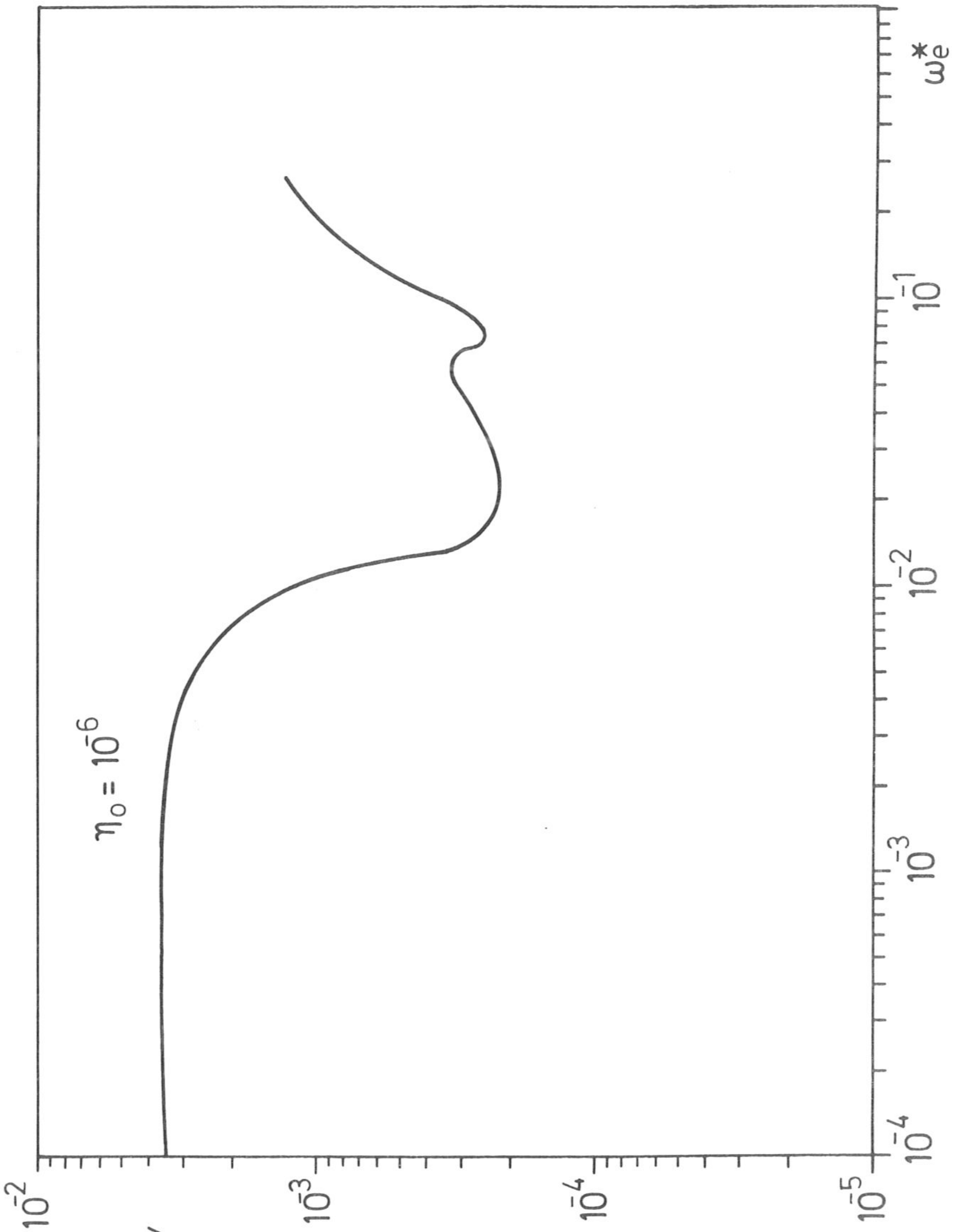

Fig. 6.

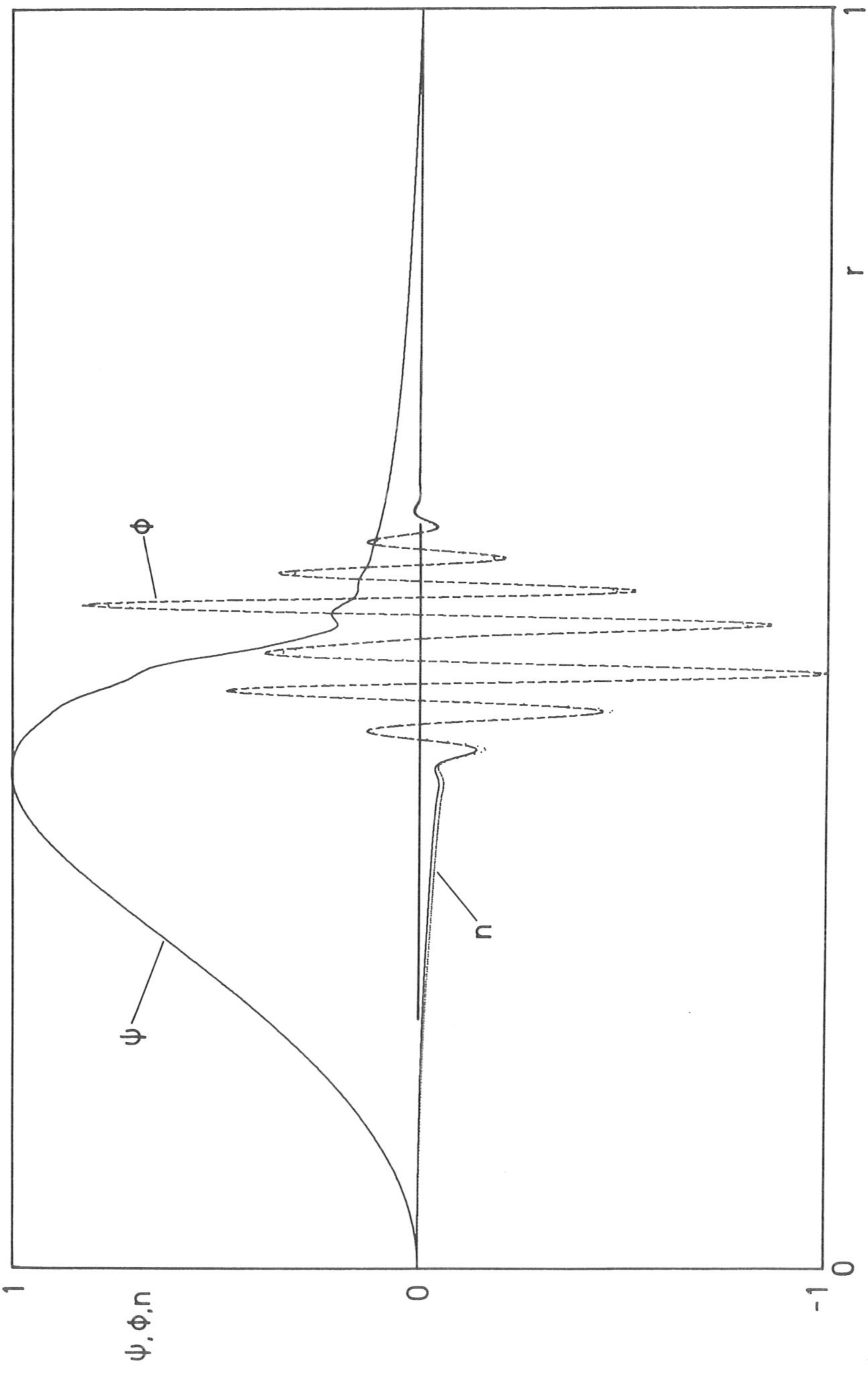

Fig. 7.

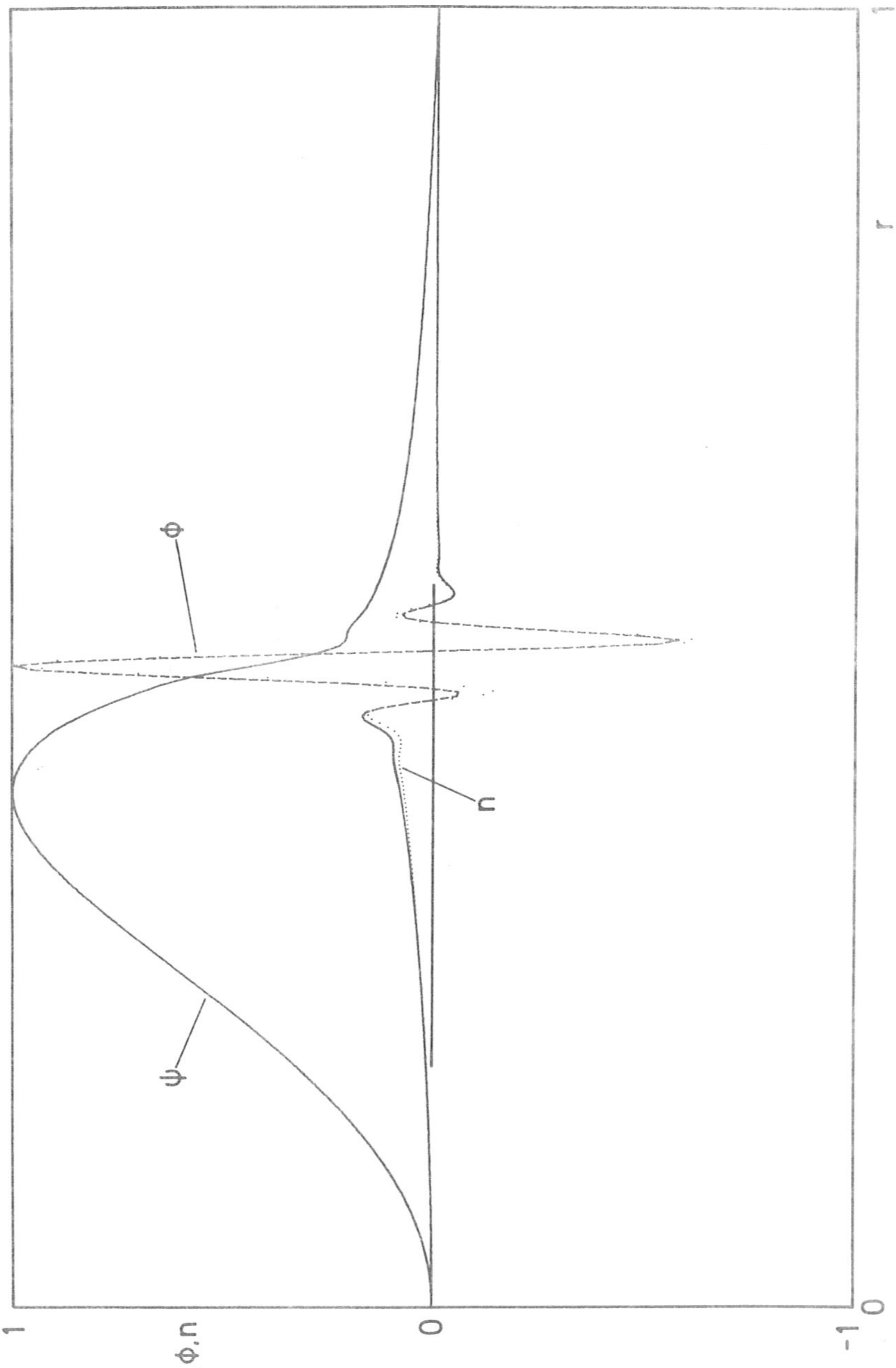

Fig. 8.

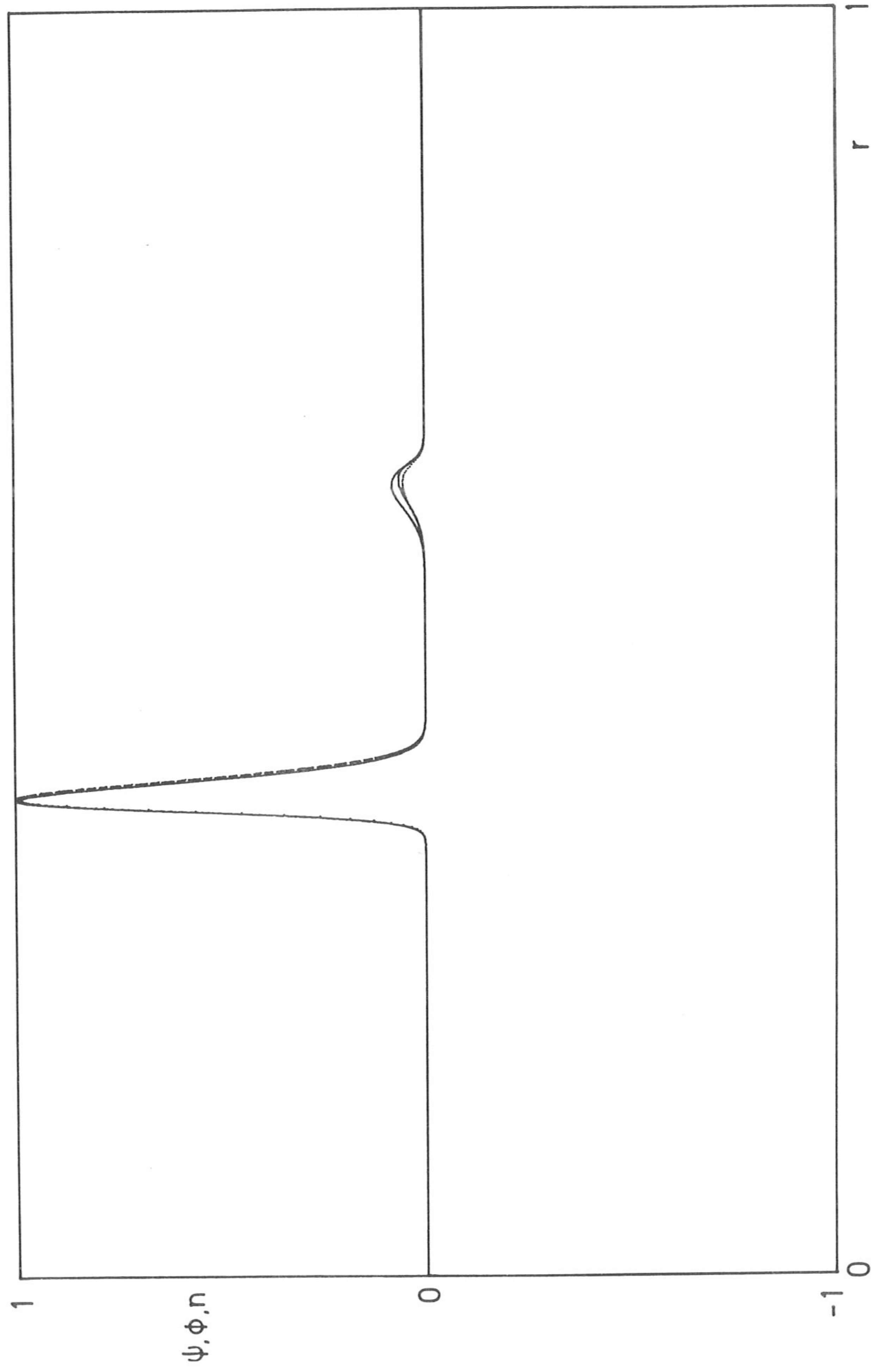

Fig. 9.

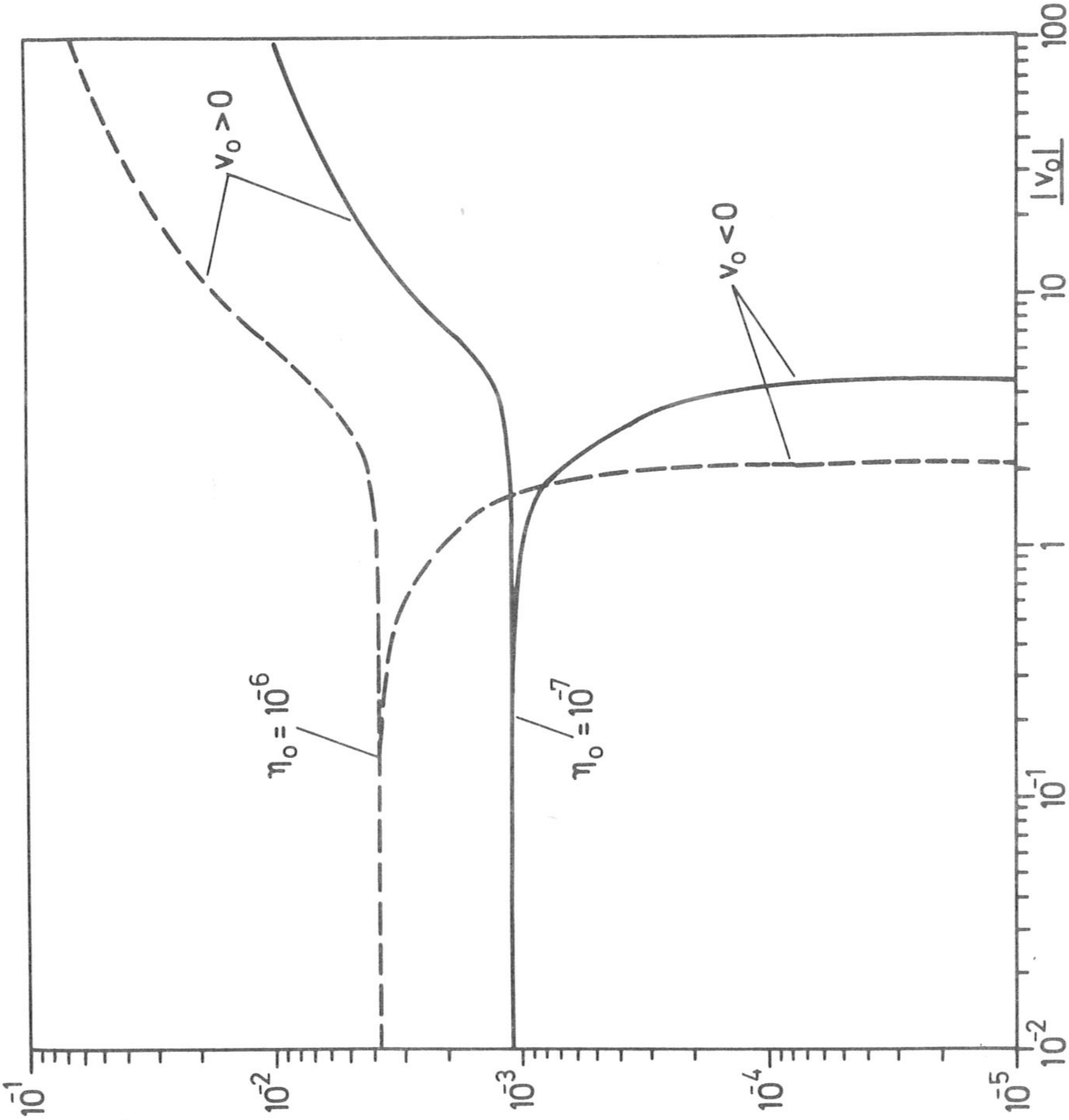

γ
$|v_o| / \eta \Delta'$
$v_o > 0$
$v_o < 0$
$\eta_o = 10^{-6}$
$\eta_o = 10^{-7}$
10^{-1}
10^{-2}
10^{-3}
10^{-4}
10^{-5}
10^{-2}
10^{-1}
1
10
100

Fig. 10.